Monatsh Chem (2014) 145:1247–1252
DOI 10.1007/s00706-014-1214-9

ORIGINAL PAPER

Phase analysis and density of the system K_2ZrF_6–K_2TaF_7

Blanka Kubíková · Jarmila Mlynáriková · Zuzana Vasková · Petra Jeřábková · Miroslav Boča

Received: 30 December 2013 / Accepted: 25 March 2014 / Published online: 24 May 2014

Abstract Thermal analysis and the Archimedean method were used to determine the phase equilibrium and density of the pseudo-binary system K_2ZrF_6–K_2TaF_7. Molar volume and excess molar volume were calculated on the basis of the experimental density data. Concentration dependencies of molar volume and molar excess volume for selected temperatures (1,133, 1,153, and 1,173 K) revealed minima at the composition $x_{K_2ZrF_6} = 0.20$. A "compressibility parameter" for K_2TaF_7 was introduced for discussion of volume changes of the system; volume contractions were observed.

Keywords Materials science · Halogenides · Thermodynamics · Phase diagrams

Introduction

The binary system K_2ZrF_6–K_2TaF_7 is the cross-section through the ternary system KF–ZrF_4–TaF_5. Investigation of the binary cross-section system seems valuable for several reasons. First, it provides the most characteristic information about the entire ternary system because it joins the two most important compounds of the corresponding binary systems KF–TaF_5 and KF–ZrF_4. Second, results will provide input data for consideration of the range of composition of a system that could also be of interest for practical applications, e.g. in the energy sector [1, 2] or for metal production [3]. Investigation of entire systems would also be valuable, but there are shortcomings that would be difficult to overcome. TaF_5 has a significantly lower melting point than ZrF_4, and binary TaF_5–ZrF_4 is disqualified for any applications because of the high price and low stability of both components. Finally, the most important motivation was to analyse the possibility of formation of a system in which a fluorine atom could serve as bridging element between two different metals.

Concerning phase diagrams, binary systems KF–ZrF_4 [4, 5] and KF–TaF_5 [3, 6–8] have been analysed several times but, despite this effort, unanswered questions remain. Also, ternary systems, in which the third component is an alkali metal fluoride, e.g. NaF–KF–ZrF_4 [9], an alkaline earth fluoride, e.g. BeF_2–KF–ZrF_4 [10, 11], or a Lewis acid, e.g. AlF_3–KF–ZrF_4 [12, 13], have been analysed, in addition to cross sections through ternary or higher systems, e.g. K_3ZrF_7–K_2BeF_4 [10, 14, 15], ZrF_4–K_2SiF_6 [16], $FLiNaK_{eut}$–K_2ZrF_6 [17], and LiF–NaF–K_2TaF_7 [18]. It is apparent the number of investigated systems and subsystems containing KF and ZrF_4 or TaF_5 as components is, surprisingly, relatively small.

Besides information on phase equilibria, volume properties of the studied melts are important. By considering deviations from ideal behaviour, e.g. volume contraction or expansion, one can deduce basic interactions in the system [19]. Unfortunately, density data are rarely available, thus systematic comparison of the investigated systems is impossible. For the systems mentioned above, data are available for $FLiNaK_{eut}$–K_2ZrF_6 [17] and KF–K_2TaF_7 [20] only. Usually, data are given in the format of an equation describing the temperature dependence of density at each composition in a specific temperature range. From such

B. Kubíková (✉) · J. Mlynáriková · Z. Vasková · P. Jeřábková · M. Boča
Institute of Inorganic Chemistry, Slovak Academy of Sciences, Bratislava, Slovakia
e-mail: uachkubi@savba.sk; blanka.kubikova@savba.sk

M. Boča
Department of Chemistry, Faculty of Natural Sciences, Constantine The Philosopher University, Nitra, Slovakia

data one can calculate the data required for other temperatures or compositions.

In this work the phase diagram and volume properties (density, molar volume, excess molar volume, and partial molar volume) of the system K_2ZrF_6–K_2TaF_7 were studied, and phases of solidified melts in the entire composition range.

Results and discussion

Phase diagram

Phase equilibria of the investigated system were determined in the entire concentration range. Temperatures of all thermal effects (T_{1-3}/K) were obtained by differentiating of the recorded cooling curves, and are summarized in Table 1. Compositions of the investigated mixtures are expressed as molar fraction of K_2TaF_7 ($x_{K_2TaF_7}$). On the basis of the evaluated temperatures of all the effects, a schematic phase diagram was constructed (Fig. 1).

The K_2TaF_7-rich side is characterized by three effects connected with the presence of this compound and its melting behaviour at high temperatures. Detailed investigation of the molten system with K_2TaF_7 has been performed several times [21–23]. It was found that K_2TaF_7 undergoes incongruent decomposition into two immiscible melts at 1,016 K and the temperature effect at approximately 979 K was attributed to the solid–solid phase transition of the K_2TaF_7. Above 1,047 K a homogenous liquid is formed. Our results are in good agreement with the previous observations, and all effects are visible on the K_2TaF_7-rich side of schematic phase diagram.

Pure K_2ZrF_6 melts incongruently [4], with the peritectic temperature $T_{per} = 859$ K. Above this temperature the system decomposes into the melt and the congruently melting K_3ZrF_7 compound with a temperature of primary crystallization of $T'_{pc} = 1{,}136$ K. However this temperature is much higher than that expected for primary crystallization on the basis of the available literature [4]. Both temperatures were recorded by thermal analysis. On addition of K_2TaF_7 to the K_2ZrF_6 it was expected the temperature of primary crystallization $T'_{pc} = 1{,}136$ K would decrease. However further thermal effects in the temperature range T'_{pc}–T_{pc} were not visible. Addition of K_2TaF_7 to the K_2ZrF_6 caused an increase of the temperature of primary crystallization. This increase was observed for the whole concentration range and the phase diagram is divided by three average temperatures $T = 911$, 973, and 1,016 K. At $T = 911$ K the compounds K_2ZrF_6, K_3ZrF_7, and K_2TaF_7 crystallize.

In the concentration range $x_{K_2TaF_7} = 0.3 - 0.8$ the lowest thermal effect indicates the area of solid–solid solution.

Table 1 Temperatures of thermal effects in the system K_2TaF_7–K_2ZrF_6

$x_{K_2TaF_7}$	T_1/K	T_2/K	T_3/K
0.00	859		1,136
0.05			861
0.10			876
0.15			885
0.20			901
0.25			911
0.30	912		925
0.35	911		933
0.40	911		948
0.45	903		950
0.50	904		959
0.55	906	967	1,014
0.60	910	966	1,018
0.65	923	974	1,026
0.70	920	980	1,032
0.75	945	984	1,034
0.80	962	994	1,042
0.85		991	1,037
0.90		1,005	1,045
0.95		1,014	1,045
1.00	995	1,016	1,047

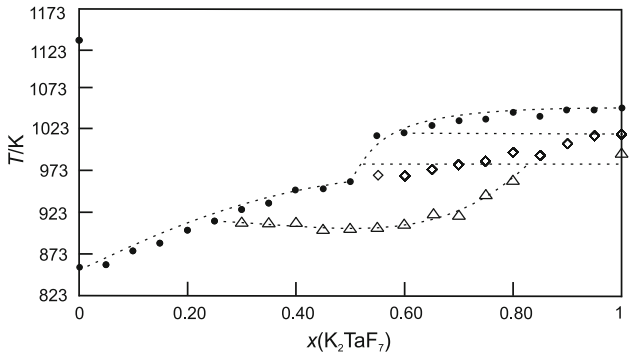

Fig. 1 Schematic phase diagram of the binary system K_2ZrF_6–K_2TaF_7; *open triangles* thermal effect T_1, *open diamonds* thermal effect T_2, *filled circles* thermal effect T_3

Solid–solid solution between K_2ZrF_6 and K_3ZrF_7 has previously been identified by Novoselova et al. [4].

Density

The temperature dependence of the density was expressed in the form of the linear equation:

$$\rho = a - bT \quad (1)$$

where ρ is density in g cm^{-3}, T is the temperature in K, and the values a and b are coefficients obtained by linear

regression analysis of the experimentally obtained data. The values of the coefficients (a/g cm^{-3}) and (b/g cm^{-3} K) together with the standard deviations of approximations (SD/g cm^{-3}) obtained by linear regression analysis of the experimentally obtained data are given in Table 2. Examples of the regression analysis for all compositions are shown in Fig. 2.

For calculation of the isothermal density and molar volume, three temperatures were selected: 1,133, 1,153, and 1,173 K. Calculated values of density based on experimental data are summarised in Table 3. Graphical representations of the concentration dependence of the density of the molten binary system K_2ZrF_6–K_2TaF_7 at the three temperatures selected, 1,133, 1,153, and 1,173 K, are shown in Fig. 3. The density increases continuously with increasing K_2TaF_7 content over the whole concentration range.

The molar volumes (V_i/g cm^{-3}) for specific compositions was calculated by use of the expression:

Table 2 Regression coefficients a and b in Eq. (1) for the temperature dependence of the density of the investigated system, K_2ZrF_6–K_2TaF_7

$x_{K_2TaF_7}$	$a \pm$ SD/g cm^{-3}	$(b \pm \text{SD}) \times 10^3$/ g cm^{-3} K^{-1}	T/K
0.00	4.312 ± 0.002	1.806 ± 0.001	1,093–953
0.20	4.755 ± 0.002	1.999 ± 0.002	1,103–1,003
0.40	4.990 ± 0.002	2.078 ± 0.002	1,273–1,033
0.60	5.325 ± 0.001	2.243 ± 0.001	1,143–1,053
0.80	5.664 ± 0.003	2.400 ± 0.003	1,213–1,133
1.00	6.154 ± 0.002	2.690 ± 0.002	1,203–1,103

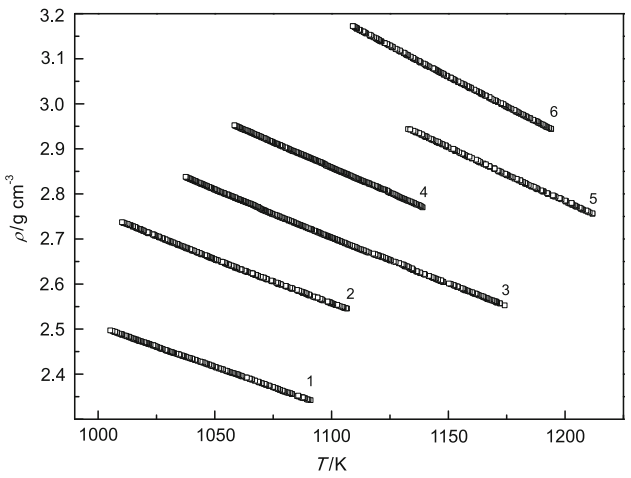

Fig. 2 Experimental results from measurement of density for all samples; *1* $x_{K_2TaF_7} = 0$, *2* $x_{K_2TaF_7} = 0.2$, *3* $x_{K_2TaF_7} = 0.4$, *4* $x_{K_2TaF_7} = 0.6$, *5* $x_{K_2TaF_7} = 0.8$, *6* $x_{K_2TaF_7} = 1$

Table 3 Calculated values of the density, ρ_i, of the molten system K_2ZrF_6–K_2TaF_7

$x_{K_2TaF_7}$	$\rho_{1,133\,K}$/g cm^{-3}	$\rho_{1,153\,K}$/g cm^{-3}	$\rho_{1,173\,K}$/g cm^{-3}
0.00	2.266	2.230	2.194
0.20	2.490	2.450	2.410
0.40	2.636	2.594	2.553
0.60	2.784	2.740	2.695
0.80	2.944	2.896	2.848
1.00	3.107	3.053	2.999

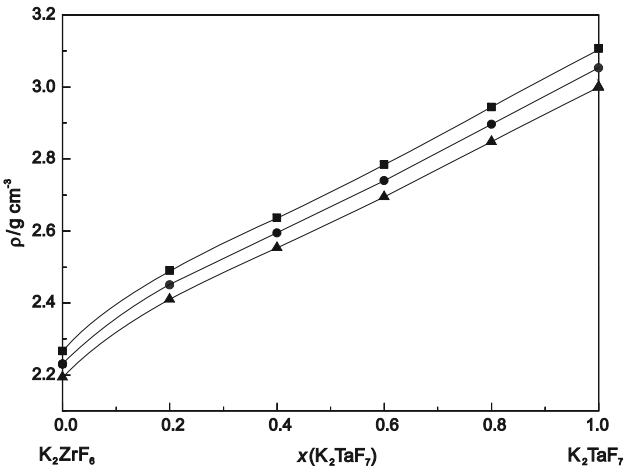

Fig. 3 Density of the molten binary system K_2ZrF_6–K_2TaF_7 at the temperatures: *filled squares* 1,133 K, *filled circles* 1,153 K, and *filled triangles* 1,173 K

Table 4 Calculated values of the molar volume, V_i/cm^{-3} mol^{-1}, of the molten system K_2ZrF_6–K_2TaF_7

$x_{K_2TaF_7}$	$V_{1,133\,K}$/cm^3 mol^{-1}	$V_{1,153\,K}$/cm^3 mol^{-1}	$V_{1,173\,K}$/cm^3 mol^{-1}
0.00	125.072	127.098	129.190
0.20	122.553	124.553	126.619
0.40	124.015	126.001	128.052
0.60	125.209	127.259	129.377
0.80	125.811	127.896	130.052
1.00	126.227	128.451	130.756

$$V_i = \frac{\sum_i x_i M_i}{\rho_i} \quad (2)$$

Calculated values of the molar volume of the molten system at the temperatures selected are summarized in Table 4 and the concentration dependence of the molar volumes at the temperatures selected are shown in Fig. 4.

The molar volume of the K_2ZrF_6 decreases after addition of the K_2TaF_7. The minimum was observed close to the composition $x_{K_2TaF_7} = 0.20$. With further addition of K_2TaF_7 the molar volume increases. This behaviour is very

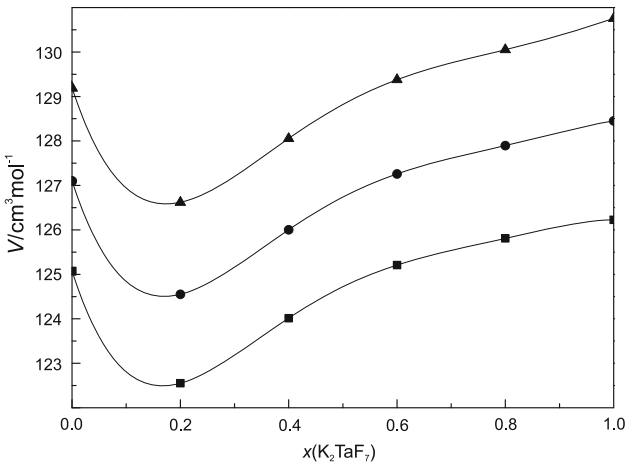

Fig. 4 Molar volume of the molten binary system K_2ZrF_6–K_2TaF_7 at the temperatures: *filled squares* 1,133 K, *filled circles* 1,153 K, and *filled triangles* 1,173 K

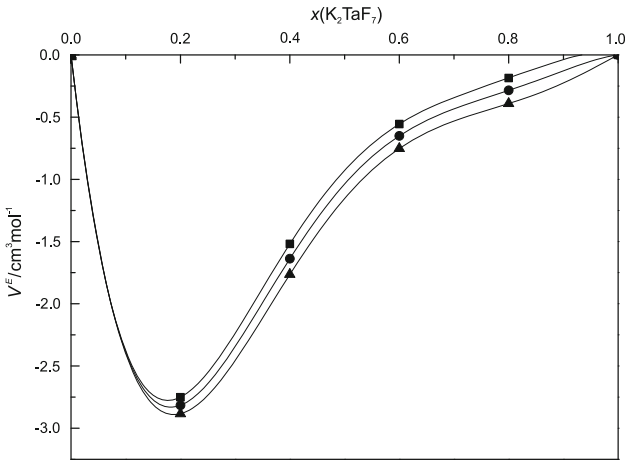

Fig. 5 Excess molar volume of the molten binary system K_2ZrF_6–K_2TaF_7 at the temperatures: *filled squares* 1,133 K, *filled circles* 1,153 K, and *filled triangles* 1,173 K

unusual. For systems reported by us [17, 19, 20, 24–28], the molar volume increased from one component to another without anomalies. For this system the initial decrease of the molar volume on addition of K_2TaF_7 up to 20 mol% must represent dramatic changes in the ionic composition and connectivity of this component. For example in the system MF–K_2NbF_7 (MF = LiF–NaF, NaF–KF, LiF–KF) it was suggested that $[NbF_8]^{3-}$ ions were formed when fluorine ions F^- coordinated with the $[NbF_7]^{2-}$ anion, and that this resulted in volume contraction. This volume contraction was identified only by monitoring excess molar volume. For the system studied in this work the volume contraction is so pronounced it is apparent even from the molar volume.

The relatively large negative deviation from ideal behaviour was observed by calculation of the molar excess volume (V^E/g cm^{-3}) of the system at the temperatures selected by use of the expression:

$$V^E = V - V^{id} = V - \sum_i V_i^* x_i \qquad (3)$$

where V/g cm^{-3} is the molar volume at the specified temperature, calculated from the measured density, V^{id}/g cm^{-3} is the ideal molar volume, x_i is molar fraction of the ith component, and V_i^*/g cm^{-3} is the molar volume of the pure ith component at the given temperature. Graphical representations of the concentration dependence of the molar excess volume of the molten binary system are shown in Fig. 5.

The dependence of molar excess volume on composition is similar to that of molar volume. Molar excess volume of the binary system K_2ZrF_6–K_2TaF_7 reaches a minimum at the composition $x_{K_2TaF_7} = 0.20$. When comparing excess molar volume for this system with data often reported for binary systems it can be seen that the minimum value of the excess molar volume for binary K_2ZrF_6–K_2TaF_7 falls within the range of minimum values of the excess molar volumes (−0.82) to (−3.25) cm^3 mol^{-1} for previously reported binary systems. The data are summarized in Table 5.

Table 5 Overview of the minima of the excess molar volumes, V^E, for previously reported binary systems

System	V^E/cm^3 mol^{-1}	References
LiF–K_2NbF_7	−0.82	[24]
NaF–K_2NbF_7	−2.5	[24]
KF–K_2NbF_7	−3.6	[25]
KF–K_2TaF_7	−3.25	[20]
$(FLiNaK)_{eut}$–K_2ZrF_6	−2.5	[17]

Dependence of molar volume on a specific composition at a given temperature can be expressed by any appropriate function. A polynomial equation of the third order was satisfied for simple fitting of the data at a given temperature. By differentiation of the polynomial equation of the third order, according to $x_{K_2TaF_7}$ and inserting into Eq. (4):

$$\overline{V}_{K_2TaF_7} = V + x_{K_2ZrF_6}\left(\frac{\partial V}{\partial x_{K_2TaF_7}}\right), \qquad (4)$$

furnished the concentration dependence of the partial molar volume of K_2TaF_7. To discuss the volume contraction and/or expansion of the system investigated in the liquid state, an excess partial molar volume or so-called "compressibility parameter", ξ, was calculated as the difference between the partial molar volume of "solute i" in "solvent" ($\overline{V}_i$/cm^3 mol^{-1}) and the molar volume of pure "solute i" (V_i/cm^3 mol^{-1}). Further information can be found elsewhere [19]. The results are summarized in Table 6.

Table 6 Volume relationships for the molten binary system K_2ZrF_6–K_2TaF_7

$V^{1,133\,K}/cm^3\ mol^{-1}$	$124.890 - 16.547x_{K_2TaF_7} + 43.173x^2_{K_2TaF_7} - 25.447x^3_{K_2TaF_7}$
$\overline{V}^{1,133\,K}_{K_2TaF_7}/cm^3\ mol^{-1}$	$126.069 + 33.168x^2_{K_2ZrF_6} - 50.894x^3_{K_2ZrF_6}$
$x_{K_2ZrF_6} \to 1; \overline{V}^{1,133\,K}_{K_2TaF_7}/cm^3\ mol^{-1}$	108.343
$(\zeta = \overline{V}^{1,133\,K}_{K_2TaF_7} - V^{1,133\,K}_{K_2TaF_7})/cm^3\ mol^{-1}$	−17.884
$V^{1,153\,K}/cm^3\ mol^{-1}$	$126.915 - 16.726x_{K_2TaF_7} + 43.388x^2_{K_2TaF_7} - 25.287x^3_{K_2TaF_7}$
$\overline{V}^{1,153\,K}_{K_2TaF_7}/cm^3\ mol^{-1}$	$128.289 + 32.474x^2_{K_2ZrF_6} - 50.574x^3_{K_2ZrF_6}$
$x_{K_2ZrF_6} \to 1; \overline{V}^{1,153\,K}_{K_2TaF_7}/cm^3\ mol^{-1}$	110.188
$(\zeta = \overline{V}^{1,153\,K}_{K_2TaF_7} - V^{1,153\,K}_{K_2TaF_7})/cm^3\ mol^{-1}$	−18.263
$V^{1,173\,K}/cm^3\ mol^{-1}$	$129.007 - 16.908x_{K_2TaF_7} + 43.591x^2_{K_2TaF_7} - 25.101x^3_{K_2TaF_7}$
$\overline{V}^{1,173\,K}_{K_2TaF_7}/cm^3\ mol^{-1}$	$130.589 + 31.711x^2_{K_2ZrF_6} - 50.201x^3_{K_2ZrF_6}$
$x_{K_2ZrF_6} \to 1; \overline{V}^{1,173\,K}_{K_2TaF_7}/cm^3\ mol^{-1}$	112.098
$(\zeta = \overline{V}^{1,173\,K}_{K_2TaF_7} - V^{1,173\,K}_{K_2TaF_7})/cm^3\ mol^{-1}$	−18.658

Table 7 Overview of values of the "compressibility parameter", ξ, calculated previously

System	$\xi/cm^3\ mol^{-1}$	T/K	References
$LiF–K_2NbF_7$	−1.96	1,273	[19]
	−2.04		
$NaF–K_2NbF_7$	−12.09	1,273	[19]
	−12.10		
$KF–K_2NbF_7$	−26.89	1,273	[19]
	−26.19		
$(FLiNaK)_{eut}–K_2ZrF_7$	−8.64	1,223	[17]
	−8.68		
$(FLiNaK)_{eut}–Na_7Zr_6F_{31}$	14.20[a]	980	[28]

The first value of the "compressibility parameter", ξ, corresponds to the first component of the binary system

[a] The "compressibility parameter" was calculated for $Na_7Zr_6F_{31}$ only

The partial molar volumes of K_2TaF_7 for each temperature are lower than corresponding molar volumes of K_2TaF_7. This means that volume contraction has occurred in the system; the magnitude of the volume contraction is from −17.884 to −18.658 $cm^3\ mol^{-1}$. These values support the statements about the changes in ionic composition in the system, although they were not apparent from thermal analysis (TA) experiments. Compared with data previously reported when volume contraction and/or expansion was discussed (Table 7), it is apparent that the "compressibility parameter" of K_2TaF_7 (Table 6) has relatively large negative value. Only for $KF–K_2NbF_7$ have we obtained more negative values. This was attributed to formation of the complex anion $[NbF_8]^{3-}$.

Conclusions

Phase equilibrium investigation of the pseudo-binary system K_2ZrF_6–K_2TaF_7 revealed several thermal effects. Two effects occurring at average temperatures $T_1 = 1{,}016$ K and $T_2 = 979$ K have been attributed to incongruent melting of K_2TaF_7. The lowest thermal effect visible in the concentration range $x_{K_2TaF_7} = 0.3 - 0.8$ indicates the presence of solid–solid solution in this range. From the experimental density data, the concentration dependence of density and volume properties was calculated for three temperatures: 1,133, 1,153, and 1,173 K. Although the density dependence increases linearly with increasing K_2TaF_7 content, local minima were observed for the molar volume and excess molar volume dependencies. Calculation of the excess partial molar volume or so-called "compressibility parameter", ξ, revealed volume contraction associated with changes in the ionic composition of the system.

Experimental

The chemicals used for preparation of the samples were: K_2ZrF_6 (Alfa Aesar, 99 %), K_2TaF_7 (prepared in the Institute of Chemistry KSC RAS, Apatity, Russia, min. 99.5 %). All salts were handled in a glove box under a dry argon atmosphere (Messer 5.0).

Phase equilibrium

The phase equilibrium of the binary system K_2TaF_7–K_2ZrF_6 was investigated by TA. The homogenized mixture (10 g) in a platinum crucible was placed in a preheated furnace (resistively heated, water-cooled, constructed at the Institute of Inorganic Chemistry, Slovak Academy of Sciences, for investigation of molten fluoride systems). Each mixture was heated and cooled in the presence of an inert gas (argon, Messer, 99.996 %). The time dependence of temperature was recorded during heating and cooling cycles. Data were collected in a LabView environment. The Pt–Pt10Rh thermocouple used for temperature determination was calibrated by means of NaCl, KF, LiF, and

NaF, all of analytical grade. Further information about the measurement procedure cas be found in our previous publications [29, 30].

Density

Density of the investigated melts was measured by use of the Archimedes method. A platinum vessel (a diameter 20 mm) suspended on a platinum wire (0.3 mm diameter) attached below an electronic balance was used as the measurement body. The dependence of vessel volume on temperature was determined by calibration using molten NaCl and KF, both of analytical grade purity. The temperature was measured by use of a Pt–Pt10Rh thermocouple calibrated in the temperature range 1,093 to 1,273 K. A PC with the LabView environment was used for control of the measurement device and for evaluation of the experimental results.

An appropriate amount of the mixture was weighed, homogenized, placed in a Pt crucible in the glove box, and then quickly transferred to the furnace. The furnace was preheated at 573 K, the position of the sample was below the measuring body, and the sample was held in an atmosphere of dried nitrogen.

Measurements were obtained in a temperature range which depended on the temperature of primary crystallization of the measured mixture. Samples were heated to the upper temperature, and the measuring body was immersed in the melts. Measurement in the cooling phase was performed to a temperature approximately 20 K above the temperature of primary crystallization. The density results were automatically recorded by the measurement device every 3 s.

Acknowledgments This work was supported by the Slovak Research and Development Agency under contract APVV-0460-10. This work was financially supported by the Scientific Grant Agency of the Ministry of Education of the Slovak Republic and the Slovak Academy of Sciences, Nos 2/0095/12 and 2/0179/10. This work is the result of the project Competence Center for New Materials, Advanced Technologies, and Energy, ITMS 26240220073, supported by the Research and Development Operational Program funded by the European Regional Development Fund.

References

1. Renault C, Hron M, Konings R, Holcomb DE (2009) The molten salt reactor (MSR) in generation IV: overview and perspectives. GIF Symposium Proceeding, Paris, p 91
2. Beneš O, Konings RJM (2008) J Alloy Compd 452:110
3. Iuchi T, Ono K (1961) Sci Rep Res Tohoku A 13:456
4. Novoselova AV, Korenev YM, Simanov YR (1961) Dokl Akad Nauk SSSR+ 139:892
5. Pauvert O, Salanne M, Zanghi D, Simon C, Reguer S, Thiaudiere D (2011) J Phys Chem B 115:9160
6. Konstantinov VI (1977) Elektrolitickoe polučenie tantala, niobija i ich splavov. Metalurgia, Moscow
7. Efros ID, Lantratov MF (1964) Zh Prikl Khim 37:2521
8. Ts'ui PH, Luzhnaya NP, Konstantinov VI (1963) Zh Neorg Khim 8:389
9. Thoma RE (1959) ORNL-2548: phase diagrams of nuclear reactor materials. Oak Ridge National Laboratory, Oak Ridge
10. Thoma RE, Insley H, Friedman HA, Hebert GM (1968) J Nucl Mater 27:166
11. Thoma RE, Insley H, Friedman HA, Hebert GM (1965) J Chem Eng Data 10:219
12. Barton CJ, Grimes WR, Insley H, Moore RE, Thoma RE (1958) J Phys Chem 62:665
13. Thoma RE, Sturm BJ, Guinn EH (1964) ORNL-3594: molten-salt solvents for fluoride volatility processing of aluminum-matrix nuclear fuel elements. Oak Ridge National Laboratory, Oak Ridge
14. Korenev YM, Novoselova AV (1963) Dokl Akad Nauk SSSR+ 149:1337
15. Chan NM, Korenev YM, Novoselova AV (1965) Zh Neorg Khim 10:1683
16. Trifonov KI, Desyatnik VN, Postnov II (1988) Rasplavy 2:125
17. Kubikova B, Mackova I, Boca M (2013) Monatsh Chem 144:295
18. Kartsev VE, Kovalev FV, Korshunov BG (1975) Izv Vuz Tsvetn Metall 3:150
19. Mlynarikova J, Boca M, Kipsova L (2008) J Mol Liq 140:101
20. Boca M, Ivanova Z, Kucharik M, Cibulkova J, Vasiljev R, Chrenkova M (2006) Z Phys Chem 220:1159
21. Netriova Z, Boca M, Danielik V, Miksikova E (2009) J Therm Anal Cal 95:111
22. Kosa L, Mackova I, Proks I, Pritula O, Smrcok L, Boca M (2008) Cent Eur J Chem 6:27
23. Kubikova B, Boca M, Gaune-Escard M (2008) Monatsh Chem 139:587
24. Chrenkova M, Cibulkova J, Simko F, Danek V (2005) Z Phys Chem 219:247
25. Chrenkova M, Danek V, Silny A (2000) Chem Pap 54:272
26. Kubikova B, Kucharik M, Vasiljev R, Boca M (2009) J Chem Eng Data 54:2081
27. Chrenkova M, Silny A, Simko F, Thonstad J (2010) J Chem Eng Data 55:3438
28. Barborík P, Vasková Z, Boča M, Priščák J (2013) J Chem Thermodyn. doi:10.1016/j.jct.2014.03.024
29. Simko F, Danek V (2001) Chem Pap 55:269
30. Chrenkova M, Danielik V, Kubikova B, Danek V (2003) Calphad 27:19